Environmental Pollution 311 (2022) 119854

Contents lists available at ScienceDirect

Environmental Pollution

journal homepage: www.elsevier.com/locate/envpol

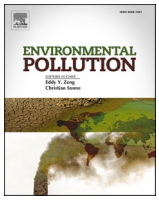

Organo-mercury species in a polluted agricultural flood plain: Combining speciation methods and polymerase chain reaction to investigate pathways of contamination☆

Lorenz Gfeller [a], Jaime N. Caplette [a], Aline Frossard [b], Adrien Mestrot [a,*]

[a] Institute of Geography, University of Bern, Hallerstrasse 12, CH-3012 Bern, Switzerland
[b] Swiss Federal Research Institute WSL, Zürcherstrasse 111, 8903 Birmensdorf, Switzerland

ARTICLE INFO

Keywords:
Methylmercury
Ethylmercury
Soil
Legacy sites
Artifacts

ABSTRACT

The analysis of organic mercury (Hg) species in polluted soils is a necessary tool to assess the environmental risk (s) of mercury in contaminated legacy sites. The artificial formation of monomethylmercury (MeHg) during soil extraction and/or analysis is a well-known limitation and is especially relevant in highly polluted areas where MeHg/Hg ratios are notoriously low. Although this has been known for almost 30 years, the thorough characterisation of artificial formation rates is rarely a part of the method development in scientific literature. Here we present the application of two separate procedures (inorganic Hg (iHg) spiking and double-spike isotope dilution analyses (DSIDA)) to determine and correct for artificial Hg methylation in MeHg-selective acid-leaching/organic solvent extraction procedure. Subsequently, we combined corrected MeHg and ethylmercury (EtHg) measurements with PCR amplification of hgcA genes to distinguish between naturally formed MeHg from primary deposited MeHg in soils from a legacy site in a Swiss mountain valley. We found the DSIDA procedure incompatible with the organomercury selective extraction method due to the quantitative removal of iHg. Methylation factors from iHg spiking were in the range of (0.0075 ± 0.0001%) and were consistent across soils and sediment matrices. Further, we suggest that MeHg was deposited and not formed *in-situ* in two out of three studied locations. Our line of evidence consists of 1) the concomitant detection of EtHg, 2) the elevated MeHg concentrations (up to 4.84 μg kg^{-1}), and 3) the absence of hgcA genes at these locations. The combination of Hg speciation and methylation gene (hgcA) abundance analyses are tools suited to assess Hg pollution pathways at Hg legacy sites.

1. Introduction

Mercury (Hg) is a pollutant of global concern due to its high toxicity and its biogeochemical cycle which spans all environmental compartments (atmosphere, oceans, soils) (AMAP/UN Environment, 2019). Relevant anthropogenic Hg sources are small scale artisanal gold mining, fuel combustion as well as the chemical industry (Horowitz et al., 2014). Sediments and soils are major Hg pools with relatively long Hg residence times (Amos et al., 2013; Driscoll et al., 2013). Legacy Hg from industrial sites (e.g. chlor-alkali plants or mining areas) retained in soils is a key source for present-day gaseous elemental mercury (GEM) in the atmosphere and a threat to downstream ecosystems due to the formation and bioaccumulation of toxic monomethylmercury (MeHg) in both aquatic and terrestrial food chains (Singer et al., 2016; Bigham et al., 2017). Fuel combustion, small-scale artisanal gold mining activities and Hg ore smelters are mainly emitting Hg as GEM. In the case of chemical plants, the speciation of the emitted Hg may often vary with the applied processes and consist of GEM, inorganic Hg (iHg) (Glenz and Escher, 2011), MeHg (Matsumoto et al., 1965), and ethyl mercury (EtHg). However, the reconstruction of Hg emissions is often difficult due to the lack of publicly available information on the pollution history. Therefore, speciation of Hg in soils may be an important tool to better understand and assess the pollution history of legacy sites.

There are many published techniques to extract and quantify organic Hg species in soils and sediments. Generally, they involve 1) an extraction step (acid, alkaline or distillation), 2) a purification

☆ This paper has been recommended for acceptance by Wen-Xiong Wang.

* Corresponding author.
E-mail address: adrien.mestrot@giub.unibe.ch (A. Mestrot).

https://doi.org/10.1016/j.envpol.2022.119854
Received 8 April 2022; Received in revised form 16 July 2022; Accepted 22 July 2022
Available online 20 August 2022

(derivatization or solvent extraction) and 3) chromatographic separation and analysis (HPLC-ICP-MS or GC-CVAFS). To date, there is no standardized technique for the quantification of organic Hg species (Hellmann et al., 2019; Jagtap and Maher, 2015).

Artificial formation of organic Hg species is one of the major problems during their extraction from soil or sediment. The formation of MeHg occurs in many extraction techniques (Hellmann et al., 2019). The first report of artificial MeHg formation dates back to the 1970s (Rogers, 1977; Rogers, 1976). Although this problem preoccupied the Hg community already in the last century (Quenvauviller and Horvat, 1999; Falter, 1999b, 1999a; Hintelman et al., 1997), no MeHg extraction technique for soil and sediment matrices has yet been proven to be free from artifact formation (Hellmann et al., 2019). The relative amounts of MeHg artifacts depend on the sample matrix (soil, sediment ect.) (Falter, 1999b; Rogers, 1977; Nagase et al., 1984; Bloom et al., 1997), the amount of leached iHg (Hammerschmidt and Fitzgerald, 2001), the pH (Rogers, 1977; Nagase et al., 1984) and the extraction solvent and method used. Published ratios of MeHg artifact formation from iHg range from 0.0003 to 0.28% in soil and sediment matrices (Bloom et al., 1997; Hintelman et al., 1997; Huang, 2005) and from 0 to 11.5% in fish tissues (Hintelman et al., 1997; Qvarnström and Frech, 2002). Table 1 summarizes the existing Hg extraction methods and their respective MeHg artifact formation. Since MeHg accounts for around 0.5–1% of the total Hg pool in background soils and sediments, these ratios result in negligible amounts of artificial MeHg formed. Polluted soils and sediments usually have very low MeHg/Hg ratios (≪0.1%) (Gray et al., 2004; Gygax et al., 2019; Xu et al., 2018) which may result in significant false positives of MeHg in polluted soils and sediments that often lead to misinterpretations (Hellmann et al., 2019). Double-spike isotope dilution analysis (DSIDA) has been successfully applied to directly quantify and correct for artificial methylation and demethylation during Hg extraction from animal tissues; however, this state-of-the-art method has shown limitations when extracting Hg from non-biological samples with high iHg concentrations (Monperrus et al., 2004; Monperrus et al., 2008). Ethyl mercury is another organic Hg species previously observed in industrial areas (Tomiyasu et al., 2017). Although, artifact formation of EtHg has rarely been reported (Huang, 2005), the detection of EtHg is not straight forward. For example, EtHg can decompose to iHg within hours under strong acidic conditions in coexistence with Fe^{3+} (Han et al., 2003), or if extracted at 60 °C in 0.1% L-Cysteine (Hight and Cheng, 2006). Further, Wilken et al. (2003) found that EtHg may have the same retention time as a certain mercury sulfur polymers (e.g. CH_3–S–Hg^+) during liquid chromatographic separation. For all the reasons stated above, it is crucial to thoroughly evaluate the analytical methods, even published and established ones, for the potential artificial formation or decomposition of the target analytes during extraction (i.e., EtHg and MeHg), before application in the field. If that cannot be avoided, a suitable and transparent method for correction must be established.

The natural formation of MeHg from iHg is mainly driven by microbial (de)methylation processes. Environments with redox oscillation (e.g., floodplains, estuaries) represent hot spots for Hg methylation (Marvin-DiPasquale et al., 2014; Windham-Myers et al., 2014; Bigham et al., 2017; Driscoll et al., 2013). Common Hg methylators are anaerobic microorganisms such as sulfate reducing bacteria (SRB), iron reducing bacteria (FeRB), archaea and some firmicutes (Podar et al., 2015). It is commonly accepted that a two-gene cluster (*hgcAB*) is responsible and essential for Hg biomethylation (Parks et al., 2013; Poulain and Barkay, 2013).

The potential for a soil net MeHg production depends on the physicochemical soil properties and Hg bioavailability (Zhang et al., 2018; Wang et al., 2021). The binding of Hg in the soil matrix has a major influence on its bioavailability and methylation. Hg in bulk sulfide particles is generally less available for methylation than if bound to sulfide nanoparticles or dissolved organic matter (DOM) (meta-cinnabar < cinnabar < Hg-DOM < Hg^{2+}) (Zhang et al., 2014; Jonsson et al., 2012). In solution, DOM promotes the dissolution and affects the crystallinity of HgS(s) phases, as well as decelerates the aggregation and growth of HgS(s) colloids. The size and structure of ß-HgS(s) and HgSe(s) particulates are hypothesized to be reciprocal to Hg bioavailability to MeHg-producing microorganisms. Further, amendments of organic matter in form of organic fertilizers enhance the net MeHg production in soils (Gygax et al., 2019).

Hg demethylation, however, is comparably less studied/understood. The most prominent pathways for MeHg decomposition are UV-light and reductive chemotrophic demethylation. For the latter, the *merB* gene was found to be essential (Parks et al., 2009). This gene is part of the mer-operon, which comprises genes encoding for Hg transport and detoxification pathways. It is also responsible for Hg reduction by the *merA* gene (Grégoire and Poulain, 2018). The abundance of *merA* linearly increases with Hg concentration in industrially contaminated soils (Osterwalder et al., 2019).

Other sources of MeHg to soil and sediments are the direct inputs of industrially contaminated materials (Matsumoto et al., 1965; Hintelman et al., 1995). In that case, we hypothesize that Hg compounds such as EtHg could be emitted alongside MeHg. The presence of EtHg in soils and sediments has been reported in different environments: remote wetlands (Mao et al., 2010), industrial areas (Tomiyasu et al., 2017; Hintelman et al., 1995), or close to volcanic activity (Tomiyasu et al., 2017). The detection of EtHg in soil from the Everglades suggests that non-anthropogenic Hg ethylation might be possible (Mao et al., 2010). However, direct, or indirect anthropogenic emissions should not be excluded. Unfortunately, no systematic studies about pathways for natural Hg-ethylation exist.

Industrially Hg polluted areas are often extensively studied in terms of contamination levels and spatial pollution extent. However, more information on the speciation of Hg could further the understanding of soil processes that cope with Hg pollution and the risks to groundwater and downstream ecosystems. Furthermore, information on Hg speciation, coupled with microbial DNA analyses, may serve as tools to determine whether organic Hg species are formed *in-situ* or directly deposited from industrial activities, and thus retrace the history of

Table 1
Methylation rates taken from the literature for various extraction methods for soils, sediments and fish tissues.

Extraction technique	Matrix	Measurement	Study	Methylation rates (%)	Reference
Distillation	sediment	GC-CV-AFS	Hg^{2+} spiking	0.036 ± 0.038	Bloom et al. (1997)
KOH/Methanol	sediment	GC-CV-AFS	Hg^{2+} spiking	0.046	
Formic Acid	sediment	GC-CV-AFS	Hg^{2+} spiking	<0.0003	
10% HCl	sediment	GC-CV-AFS	Hg^{2+} spiking	<0.002	
KOH/CH_2Cl_2	sediment	GC-CV-AFS	Hg^{2+} spiking	0.022 ± 0.021	
KBr/H_2SO_4/$CuSO_4$	sediment	GC-CV-AFS	Hg^{2+} spiking	0.0025 ± 0.0013	
TMAH	fish tissue	HPLC-ICP-MS	SS-ID	0.1–11.5	Qvarnström and Frech, 2002
TMAH/Ethylation	sediment	GC-ICP-MS	SS-ID	0.03	Hintelman et al., 1997
5M HCL/Toluene	sediment	HPLC-ICP-MS	SS-ID	0.005	
TMAH/Ethylation	fish tissue	GC-ICP-MS	SS-ID	4.3	
Distillation	fish tissue	HPLC-ICP-MS	SS-ID	no MeHg formation	
$CaCl_2$/Tropolene/Acetic acid/Propylation	soil	GC-ICP-MS	Hg^{2+} spiking	0.03–0.28	Huang, 2005

pollution in the area. We hypothesize that the absence of *hgcA* in a soil sample with a high MeHg concentration would suggest that this MeHg was deposited and not formed *in-situ*, since the *hgcAB* gene cluster is essential for the biomethylation of Hg. This hypothesis can be further strengthened by the presence or absence of other organic Hg species such as EtHg.

In this study, we tested, improved, and applied a previously published high-throughput extraction method for organo-Hg species (MeHg and EtHg) and analysis by high performance liquid chromatography-inductively coupled plasma-mass spectrometry (HPLC-ICP-MS) in less than 7 min (Brombach et al., 2015; Sannac et al., 2017; Gygax et al., 2019). We analyzed 163 samples from polluted agricultural floodplain in an alpine mountain region. We aimed to precisely quantify the artificial methylation of Hg during extraction to correct for false positives using two different methods (iHg spiking and DSIDA). We successfully corrected for artificial Hg methylation and discussed the advantages and disadvantages of the two methods tested. Subsequently, we characterized the soils from the legacy site and assessed its pollution history.

2. Methods and materials

2.1. Sample location, sample collection, sample processing

Soil samples were collected between April and May 2017 from an agriculturally used floodplain between Visp (N 46°17′58.780″; E 7°51′06.369″) and Niedergesteln (N 46°18′46.464″; E 7°46′54.455″), Wallis, Switzerland (Fig. S1). The site is situated downstream from an acetaldehyde and chlor-alkali chemical plant and is historically affected by Hg pollution. The Hg was released from the plant through a wastewater discharge canal between 1931 and 1976. The canal sediments were used as fertilizer on the canal's bank and across the agricultural fields between the 1960s and 1980s. Further contaminated materials were used to fill pits and construct terrain modifications in the floodplain (Mudry, 2016). The reported Hg concentrations in the soils from this area range from 0.5 to 470 mg kg^{-1} (Mudry, 2016; Gilli et al., 2018; Gygax et al., 2019) and atmospheric emissions of GEM have been documented at this site (Osterwalder et al., 2019; Glenz and Escher, 2011 and references there in). For this study, three sites with elevated Hg levels were chosen based on a preliminary Hg-screening campaign (Dienststelle für Umwelt, 2016). Soils were sampled within a rectangular grid (25 × 20 m) divided into 25 m^2 squares. Following this scheme, a total of 12 soil cores were taken using a Pürckhauer corer with a target depth of 50 cm and divided into 10 cm intervals (Fig. S2). Sites were named Canal Site, Landfill and Hotspot after their geographical location (Table S1) or previously measured Hg concentrations.

Samples were double bagged in polyethylene (PE) bags. The sample bags were stored on ice immediately then frozen (−20 °C) at most 8 h after sampling. A selection of fresh samples for DNA extraction was kept in at −20 °C in extraction buffer using the DNeasy® PowerSoil® Kit (QIAGEN, Venlo, NL) until DNA extraction. In the laboratory, the remaining material was freeze-dried, sieved to <2 mm grain size, and ground using an agate mortar. In soil and sediment matrices, freeze drying was demonstrated to affect Hg concentration and speciation the least when compared to oven drying (Hojdová et al., 2015). The processed samples were stored at room temperature until analysis.

2.2. Materials and reagents

HPLC grade solvents and ultra-pure water (MilliQ, >18.2 MΩ cm at 25 °C) were used. Acids (HNO_3, HCl) were doubly distilled in our in-house clean lab. Glassware was cleaned by soaking in acid baths (both 10% (w/w) HNO_3 and 10% (w/w) HCl) for at least 24 h and rinsed with ultra-pure water. Corning® sterile polypropylene (PP) tubes were used to store digests for of total Hg and trace metal analyses. Borosilicate glassware was used for MeHg extractions and storage. Commercially available stock solutions for multi-element (ICP multi-element standard solution IV-ICPMS-71A, Inorganic Ventures, Christiansburg, United States of America) and total Hg (ICP inorganic Hg standard solution, TraceCERT®, Sigma-Aldrich, St. Louis, United States of America) analyses were used as standards. MeHg standards were prepared by dissolving MeHg chloride (Sigma-Aldrich, St. Louis, United States of America) in methanol (HPLC grade, Fisher Scientific, Reinach, Switzerland). The EtHg standard solution was kindly provided by Prof. Milena Horvat (Laboratory of the Department of Environmental Sciences, Jožef Stefan Institute Ljubljana, Slovenia). Commercially available isotopically enriched standards of ^{199}iHg and ^{201}MeHg (Enriched Standards, ISC Science, Oviedo, Spain) were used for DSIDA. Working solutions for analyses were prepared daily by gravimetric dilution using the analyte-specific solvents. All samples, standards and spikes were weighed with an analytical balance (ALJ 220-4, Kern & Sohn GmbH, Balingen, Germany) to a precision of 10^{-4} g.

2.3. Standard soil parameters

All soils were analyzed for pH, carbon (C), nitrogen (N), sulfur (S), soil organic carbon (SOC) and the metals relevant for Hg cycling in soil (i.e., Fe, Cu and Mn). Soil pH was measured in an equilibrated 0.01 mol L^{-1} $CaCl_2$ solution (1:5 soil:liquid ratio) using a pH probe (SenTix® 41, WTW, Weilheim, Germany). Soil CNS was measured with an elemental analyzer (vario El cube, Elementar Analysensysteme, Germany). SOC was calculated by the difference in C concentration before and after a thermal loss on ignition (LOI) treatment at 550 °C for 2 h. Soil metals were leached by microwave-assisted acid digestion (250 mg soil, 4 mL 69% (w/w) HNO_3, 2 mL 30% (v/v) H_2O_2). The soils trace and major metals (in 1% HNO_3) and Hg (in 1% HNO_3, 0.5% HCl) concentrations were quantified by inductively coupled plasma-mass spectrometry (ICP-MS; 7700x ICP-MS, Agilent Technologies, Santa Clara, United States of America). An internal standard of indium (m/z 115) was continuously injected through the peristaltic pump using a T-piece. The ICP-MS operating conditions for multi-element and Hg analyses are shown in Table S2. The rinsing protocol shown in Table S3 was used during HgT analyses to avoid memory effects. The limit of detection (LoD) for Hg in soil solution was <0.02 μg kg^{-1} for all soil analyses. Soil digestions and extractions were verified using the certified reference materials (CRMs) SRM 2s709a (San Joaquin Soil, National Institute of Standards and Technology, Gaithersburg, USA), PACS-3 (Marine sediment, National Research Council of Canada, Ottawa, Canada) and ERM-CC580 (Estuary sediment, Institute for Reference Materials and Measurements, Geel, Belgium). The recoveries of multi-element, Hg and MeHg of CRMs are shown in Table S4. For a selected set of samples soil grain size distribution was analyzed. Samples (sieved <2 mm) were treated with 30% (v/v) hydrogen peroxide (H_2O_2, Sigma-Aldrich, St. Louis, United States of America) to remove SOM and dispersed in a solution of 22 mM sodium carbonate and 18 mM sodium hexametaphosphate. Particle-size composition was measured using a MasterSizer 2000 (Malvern Panalytical Ltd., UK).

2.4. Organic Hg speciation analyses

2.4.1. Extraction

We modified a published method for high sample throughput (up to 64 samples per extraction batch) in 8 h for the extraction of organic Hg species (Gygax et al., 2019; Brombach et al., 2015). Briefly, 0.25 g of sample was suspended with 10 mL of a 6 mol L^{-1} HCl solution in a 20 mL borosilicate glass vial (Fig. S3). After 30 min of overhead shaking, the vial was centrifuged for 3 min at 680×*g* and the supernatant was decanted. Then, 5 mL of CH_2Cl_2 (dichloromethane or DCM, Fisher Scientific, Reinach, Switzerland) was added to the extract, shaken for 60 min to extract organic Hg species and transferred to a borosilicate glass vial. Then, 2 mL of a 0.1% (w/v) L-cysteine aqueous solution were added. For the back-extraction, the organic solvent was evaporated with a constant flow of N_2 at 50 °C. The amount of L-cysteine solution was weighed at

every step to account for loss by evaporation. The extracts were stored in the dark at 4 °C and analyzed within 48 h. To assess MeHg extraction efficiency, we used a CRM ERMCC-580 (68 ± 2 μg kg^{-1}, recovery = 90.8%, n = 39, Table S4) for MeHg recoveries. To date, there is no suitable CRM available for EtHg for validation of EtHg extractions. Measured EtHg concentrations were interpreted as minimum concentrations in a sample, due to reported degradation of EtHg to Hg during acidic extractions using HCl (Duan et al., 2016) or extractions involving heating at 60 °C in 0.1% (w/v) L-cysteine (Hight and Cheng, 2006). Degradation of EtHg was not reported to produce interference with MeHg for the speciation analysis method used (Hight and Cheng, 2006).

2.4.2. HPLC-ICP-MS analyses

After extraction, Hg species were separated and analyzed using a previously published method (Sannac et al., 2009; Gygax et al., 2019; Sannac et al., 2017) by coupling a high performance liquid chromatograph (HPLC 1260 Series, Agilent Technologies, Santa Clara, United States of America) to the ICP-MS (HPLC-ICP-MS). We used a reversed phase C18 column (Zorbax C-18, 4.6 × 50 mm, Agilent Technologies, Santa Clara, United States of America) and a mobile phase consisting of 0.1% (w/v) L-cysteine (98% v/v) and methanol (2% v/v). The detailed HPLC operation conditions are given in Table S5. The LoD was calculated from the daily calibration curve and was <0.14 μg kg^{-1} in soil samples. Three Hg species (Hg^{2+}, $MeHg^{+}$ and $EtHg^{+}$) were separated within 7 min under isocratic conditions (Figs. S4–S5).

2.4.3. Quantification of methyl mercury artifacts

Two approaches were chosen to quantify the formation of artificial MeHg during the extraction of organic Hg species.

As a first approach, we used a double-spike isotope dilution analysis (DSIDA) (Monperrus et al., 2008). Briefly, 0.25 g of sample were weighted into the glass vial and spiked with both isotopically enriched ^{199}MeHg and ^{201}iHg to achieve isotope ratios (^{199}Hg/^{202}Hg for MeHg and ^{201}Hg/^{202}Hg for iHg) in the range of 0.8–1.5. The spike and the samples were mixed for 30 min by overhead shaking. Then, the soils were extracted according to the method in section 2.3. This procedure did not compensate for non-quantitative extraction or speciation changes during the acid leaching step by HCl due to the relatively short equilibration time between solid and spike. However, it reduced the risk of speciation changes of the spiked material prior to the extraction. The samples were then analyzed by HCPL-ICP-MS as in section 2.4.2. A Tl internal standard solution was continuously introduced through the peristaltic pump using a T-piece. Mass bias was corrected with ^{203}Tl/^{205}Tl ratios during each measurement. The instrument setup used for isotope dilution analysis by HPLC-ICP-MS can be found in Table S6. The analyzed isotopic ratios ($R_{MeHg}^{202/201}$, $R_{MeHg}^{202/199}$) allowed for the quantification of MeHg using the classic isotope dilution approach (Eq. (1)) (Monperrus et al., 2004 and references cited therein):

$$c = \frac{c' w' A_r (RY' - X')}{w A_r' (X - RY)} \quad (1)$$

where c = concentration of sample; w = mass of sample; A_r = relative atomic mass of the element (or species) being determined; X = isotopic abundance (atom-%) Hg^{202}; and, Y = isotope abundance (atom-%) Hg^{199}. Correspondingly for the spike, c' = concentration of the spike; w' = mass of the spike; A_r' = relative atomic mass of the element (or species) in the spike; X' = isotopic abundance (atom-%) Hg^{202}; and, Y' = isotope abundance (atom-%) Hg^{199}. The parameters analyzed by HPLC-ICP-MS are therefore R (here $R_{MeHg}^{202/199}$). The other parameters are constants or masses weighed with analytical balances to a precision of 10^{-4} g.

The enriched ^{201}iHg spike was used to quantify the methylation factor ($F_{methylation}$). It was calculated with the equation (Eq. (2)) developed by Monperrus et al. (2008). The authors used ^{201}MeHg and ^{199}iHg spikes. We adopted these equations to our ^{199}MeHg and ^{201}iHg spikes (Enriched Standards, ISC Science, Oviedo, Spain).

$$F_{methlyation} = \frac{N_{sp}^{MeHg}}{N_{sp}^{IHg}} \times \frac{\left[\frac{\left(At_{sp,MeHg}^{202} - R_{MeHg,\,m}^{202/199} At_{sp,MeHg}^{199}\right)}{\left(R_{MeHg,m}^{202/199} At_s^{199} - At_s^{202}\right)} - \frac{\left(At_{sp,MeHg}^{202} - R_{MeHg,\,m}^{202/201} At_{sp,MeHg}^{201}\right)}{\left(R_{MeHg,m}^{202/201} At_s^{201} - At_s^{202}\right)}\right]}{\left[\frac{\left(At_{sp,IHg}^{202} - R_{MeHg,\,m}^{202/201} At_{sp,MeHg}^{201}\right)}{\left(R_{MeHg,m}^{202/201} At_s^{201} - At_s^{202}\right)} - \frac{\left(At_{sp,IHg}^{202} - R_{MeHg,\,m}^{202/199} At_{sp,MeHg}^{199}\right)}{\left(R_{MeHg,m}^{202/199} At_s^{199} - At_s^{202}\right)}\right]} \quad (2)$$

The selective extraction of organic Hg species did not allow for the complete correction proposed by Monperrus et al. (2008). The authors used $R_{iHg}^{202/201}$ and $R_{iHg}^{202/199}$ to correct for MeHg demethylation during the experiments. However, iHg was not consistently detected using our selective extraction procedure.

The second approach was spiking soil samples with a standard of iHg as 1000 mg Hg L^{-1} before extraction (see Sect. 2.3). This was done at three different spike levels to meet ratios of 2:1,1:1,1:2 with respect to the amount of Hg leached by HCl. The experiment was conducted using two paddy soil samples from our sample bank, a contaminated sediment standard material (ERM-CC 580), and a blank without a soil or sediment matrix. In the blank samples, we spiked four different levels in the range of 6.4–51 μg. After extraction, the samples were analyzed by HPLC-ICP-MS. The measured MeHg concentrations were compared to MeHg concentrations recovered without addition of iHg spikes. Here the methylation factor ($F_{methylation}$) was calculated as the slope of the linear model between $MeHg_{measured} \sim (Hg_{spiked} + Hg_{ambient})$. This linear model is shown in Eq. 3

$$MeHg_{present} = MeHg_{measured} - F_{methylation} * \left(Hg_{spiked} + Hg_{ambient}\right) \quad (3)$$

Calculated values of $Hg_{ambient}$ were used to correct for the artificially produced MeHg (see Sect 3.1). This was done by HCl leaching, which directly corresponds to the first step of the organo-Hg extraction procedure. The HCl extracts were measured for total Hg using ICP-MS by a set of standards calibrations. Corrections for both experimental approaches were done using Eq. (4).

$$MeHg_{corrected} = MeHg_{measured} - F_{methylation} * Hg_{HCl-leached} \quad (4)$$

2.5. Microbial DNA extraction and hgcA gene amplification

Total genomic DNA was extracted from 0.25 g of fresh soil sieved at 2 mm using the DNeasy® PowerSoil® Kit (QIAGEN, Venlo, NL) and following manufacturer recommended protocol. DNA concentrations were determined using PicoGreen (Molecular Probes, Eugene, OR, USA). Polymerase chain reaction (PCR) of the hgcA gene was performed using the primers hgcA_262F and hgcA_941R as described in (Liu et al., 2018). The presence or absence of the amplified hgcA gene in the soil samples was visually verified by the absence or presence of a specific band corresponding to the amplification length (315 bp) on the gel.

2.6. Statistics

Plotting, data treatment, calculations and statistical analyses (linear regressions and correlation coefficients) were conducted with R Studio (RStudio Team, 2020) using the packages “tidyverse”, “HMisc” and “corrplot”. Mean concentrations and percentual recoveries are given with an uncertainty of one standard deviation for samples extracted in triplicates (mean ± 1*σ). For the linear regressions we give the squared Pearson’s correlation coefficient (r^2) and p values with a cut-off at ($p < 0.05$). Correlation matrices of all assessed parameters, aggregated by site are given in Figs. S6–S8.

3. Results and discussion

3.1. Soil properties and distribution of contaminants

During the field campaign, we sampled soil from three sites in a contaminated agricultural area in the canton of Wallis, Switzerland. The

canal site was situated on an agricultural field cultivated with corn for the past three years. The soil at this site was classified as *fluvi gleyic anthrosol* (IUSS Working Group WRB, 2015), and showed a clear ploughing horizon (Ap) at a depth of 30 cm with very few soil aggregates with no meso- or macrofauna spotted during sampling. The Ap horizon is followed by a horizon with gleyic properties between 30 and 50 cm depth featured by red and black redoximorphic features (interpreted as Fe and Mn oxides) and a layered sandy texture that indicates fluviatile influence (Fig. S9). Chemical and physical soil parameters are given in Table S7. According to public records, Hg contaminated canal sediments heavily affected the pollution of soils at the borders of the discharging canal (Grossgrundkanal) (Glenz and Escher, 2011). At this site, Hg concentrations show both a horizontal gradient perpendicular to the canal as well as a sharp decrease at a depth of 30 cm (ploughing horizon). The horizontal gradient indicates a continuous physical transport of the contaminated material from the initially contaminated bank to the agriculturally used field. For the sampled soil, Hg correlates with the clay grain size ($R^2 = 0.7$, $p < 0.001$), which was described earlier at the same legacy site (Gygax et al., 2019). A sharp vertical decrease in Hg coincides with a change in the grain size distribution between 30 and 40 cm (Fig. 1). This textural change is clearly visible in the sampled cores and marks the Ap horizon of the agricultural field (Fig. S9). These observations suggest that the bulk Hg pool is mainly transported by anthropogenic processes (e.g., ploughing). However, Hg was shown to be mobilized and transported in the aqueous phase (e.g., thought reductive dissolution of Mn oxides associated with Hg) and advective transport (Gfeller et al., 2021; Gygax et al., 2019; Gilli et al., 2018; Frossard et al., 2018).

At the canal site, soil Hg concentrations positively correlate with other chalcophile metals such as Cu ($R^2 = 0.54$, $p < 0.001$), Zn ($R^2 = 0.88$, $p < 0.001$) and Pb ($R^2 = 0.79$, $p < 0.001$) (Fig. 2, Fig. S10). Co-occurrence of Hg with higher levels of Zn and Cu has been documented earlier in industrial legacy floodplain soils (Lazareva et al., 2019). This suggests that the canal sediment is a common source of these metals in the contaminated soil, although they get there through different pathways. Among others, inputs of Zn and Cu in agricultural soils come from the application of organic fertilizers (Imseng et al., 2019; Mantovi et al., 2003) or fungicides. Further, Pb is immobile under high pH conditions and originates from tire abrasion, mining or shooting activities. We suggest that the historically polluted canal sediments (Glenz and Escher, 2011) represent the source of Hg, Zn, Cu and Pb in the soil at this site given the shared special gradient (distance from canal) and the good correlation between them. More data along the canal site is needed to further evaluate Pb, Cu, and Zn as proxies for Hg levels at this specific site. Earlier studies reported that Hg was mainly present as HgS in the recalcitrant fraction of sequential extractions and less as bound to Mn oxyhydroxides and NOM in contaminated soils of the area (Grigg et al., 2018). Also, Hg bound to Mn oxyhydroxides were reported as relevant pools for remobilization of soil bound Hg to the aqueous phase (Gilli et al., 2018; Gfeller et al., 2021). In summary, we show indications that the bulk Hg pool is mainly present in a fine grain size fraction together with other metals often bound to sulfides (e.g., Cu, Zn and Pb).

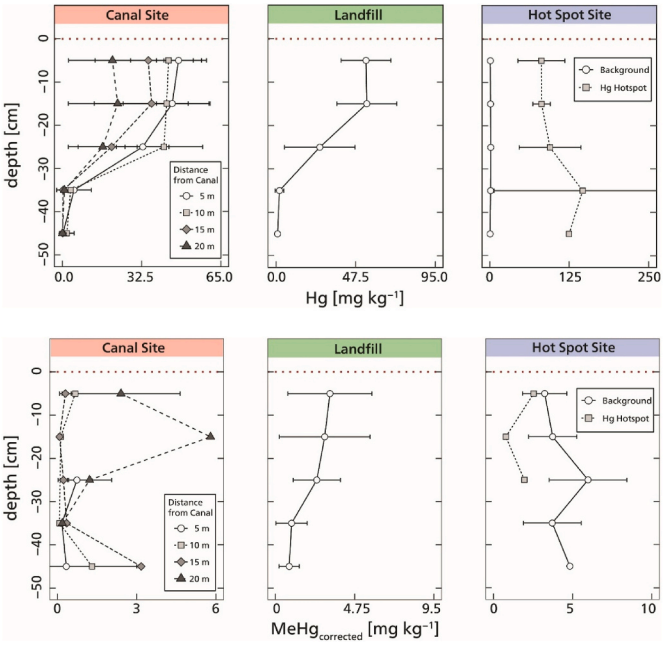

Fig. 1. HgT and corrected MeHg concentrations of the soil profiles at each site. Points represent the mean; error bars represent one standard deviation of soil HgT concentrations. For the canal site the data was aggregated to the distance from the canal bank of the Grossgrundkanal. For the Hot Spot Site data was aggregated according to cores within the Hg hotspot and cores outside of the Hg hotspot.

The landfill site situated on the agricultural area is around 500 m away from the discharging canal (Fig. S1). High Hg levels were already measured earlier at this site (Dienststelle für Umwelt, 2016). However, the source and history of pollution at this site is not completely documented (Glenz and Escher, 2011). The soil was classified as a *toxic Technosol* (IUSS Working Group WRB, 2015) consisting of a single Au horizon (0–50 cm) (Fig. S4) with a silty sand texture consistent with depth. SOC decreases from 2.1 ± 0.3% to 0.9 ± 0.8% and the pH varied between 8.17 and 7.30 without horizontal trends. During the sampling, we did not spot macrofauna. At increasing depth, Hg gradually decreases from approximately 50 mg kg^{-1} to 25 mg kg^{-1} between 0–30 cm and to <5 mg kg^{-1} below 30 cm (Fig. 1). As for the canal site, Hg concentrations positively correlates with Cu ($R^2 = 0.46$, $p < 0.001$) and Pb ($R^2 = 0.83$, $p < 0.001$), although that correlation was weaker for Zn and Hg ($R^2 = 0.26$, $p < 0.001$) (Fig. 2).

The hot spot site is situated in the vicinity of a farm on a pasture field. High Hg concentrations (>20 mg kg^{-1}) were reported earlier at this site (Dienststelle für Umwelt, 2016). The soils parental material was heterogenous within the sampled grid. Due to detected anthropogenic artifacts and the high Hg concentration (see section 3.2), the soil at this site was also classified as a *toxic Technosol* (IUSS Working Group WRB, 2015). We observed variations from high amounts of soil skeleton to its complete absence (⌀ > 2 mm, gravel and angular rock pieces). Cores could not be fully retrieved (0–30 cm) in profiles with high amounts of gravel. Some profiles showed sharp changes between gravel-rich material and sandy material. Anthropogenic artifacts (e.g., metal shavings) were identified in some cores. The fine soil (⌀ < 2 mm) showed a silty sand texture consistent with depth. All profiles expressed a thin A-horizon (approximately/c.a. 5 cm) indicative for a recent onset of soil development. SOC decreases sharply between 0 and 10 cm (from 4 ± 1 to 3.0 ± 0.7 wt %) and then gradually without distinct horizontal trends to 1.0 ± 0.6 wt % at 50 cm depth. Soil pH was in the neutral range (6.51–7.87) and showed no spatial gradients. The heterogeneity of the soil skeleton is indicative of glacial fluvial or anthropogenic deposition of the parent material. The placement of the sampling grid did not allow for the full coverage of the previously reported hot spot by a sampling campaign of the local authorities (Dienststelle für Umwelt, 2016). We detected high Hg concentrations (47.5–244.8 mg kg^{-1}) in two soil cores at the NE edge of the grid, which represents a Hg hotspot (Fig. 1). The cores around the hot spot still showed elevated Hg concentrations (0.02–3.92 mg kg^{-1}) when compared to the European background of 0.023 mg kg^{-1} (Panagos et al., 2021). Similarly to the other two sites, Hg concentrations positively correlated with Cu ($R^2 = 0.69$, $p < 0.05$) and Pb ($R^2 = 0.57$, $p < 0.05$); but there was no relationship between Zn and Hg (Fig. 2). There is an indication for a common source of the contaminated material at all studied sites given by the common linear relationships between relatively immobile trace elements (Cu, Pb, Hg). However, analysis of organic Hg species could help to better understand

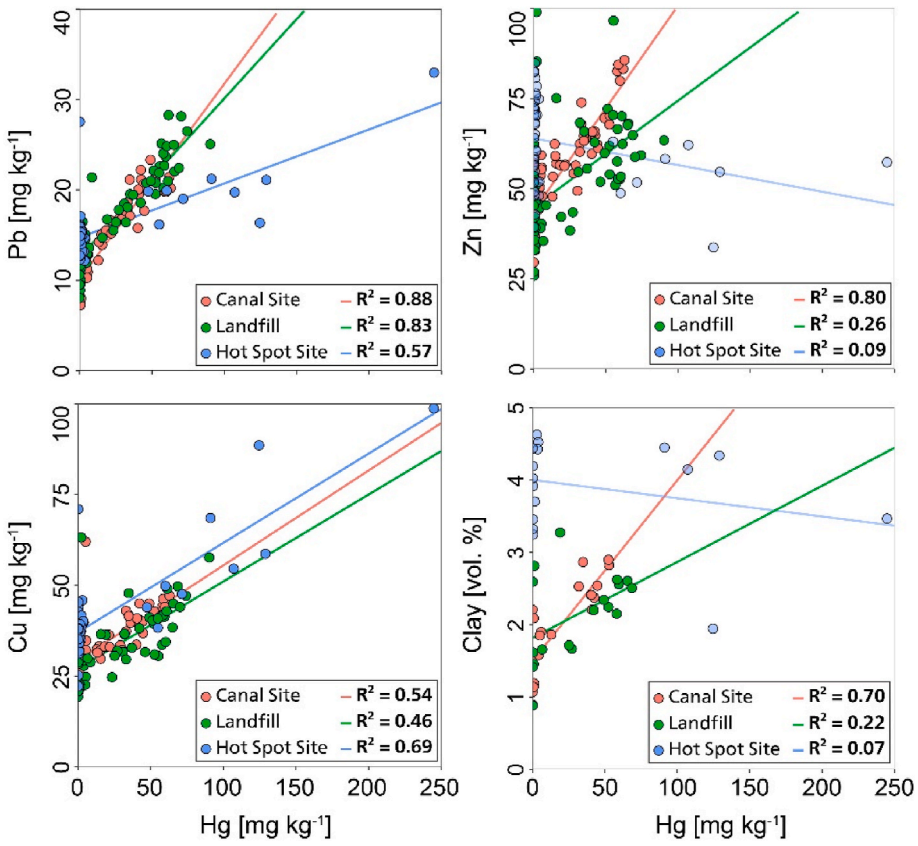

Fig. 2. Scatterplot displaying relationships between soil HgT and Pb, Cu, Zn concentrations and clay percentage for the canal site (red), landfill site (green), and hot spot site (blue). Lines show the fitted linear regression models at each site. (For interpretation of the references to colour in this figure legend, the reader is referred to the Web version of this article.)

the history and the source material of these contaminated sites as well as processes involved in the formation of these species in soil. For that we tested and validated an analytical method for the determination of organic Hg species in soil.

3.2. Methylmercury extraction method development

Validated high throughput MeHg extraction methods are needed to monitor MeHg and study (de)methylation processes in highly contaminated areas. Here, we optimized the HCl– Cl_2CH_2 extraction procedure by Brombach et al. (2015) to extract 64 samples per day. This method was chosen since it allows for selective extraction of MeHg, which is important in soils where most of the Hg is iHg. Also, the extracts can be directly measured by HPLC-ICP-MS. Further, we tested the method for net artificial MeHg production in blanks and soil matrices. This was especially important in the scope of earlier studies using HCl extractions reporting insufficient quantitative leaching (Horvat et al., 1993), MeHg decomposition above 4 mol L^{-1} HCl (Horvat et al., 1993) or the artificial methylation of iHg (Hintelman et al., 1997) in sediment and soil matrices. To our knowledge, no such tests have yet been published for this specific soil and sediment extraction procedure. During the test phase, we did not observe MeHg when directly injecting 10 μg L^{-1} iHg into the HPLC-ICP-MS and conclude that no significant amounts of MeHg are produced during the actual analysis. Thus, the extraction procedure accounts for any artificial MeHg formation observed in the following tests.

3.2.1. Experiment A - artificial methylation: species specific isotope dilution approach

For the isotopic dilution experiment, we analyzed one top-soil sample in triplicate (0–10 cm) from each site (canal, landfill and hot spot) as well as the CRM ERM CC-580 in triplicate. During the selective extraction, iHg was highly variable in the analyzed extract since it was mainly partitioning in the HCl (Fig. S11). Therefore, Hg^{2+} could not be analyzed for target isotopes (^{199}Hg, ^{201}Hg, ^{202}Hg).and demethylation of MeHg ($F_{demethylation}$) was not quantified by DSIDA equations due to the low iHg signals. However, Monperrus et al. (2008) reported issues with the quantification of $F_{demethylation}$ due to the overestimation of the demethylation of $^{199}MeHg$ to ^{199}iHg in the presence of high natural iHg levels during the acid-leaching derivatization procedure. Therefore, MeHg concentrations were calculated with the classical isotope dilution equation (IDA) (Eq. (1)). Independently, methylation factors ($F_{methylation}$) were calculated according to Eq. (2). Then, separately analyzed iHg concentrations were used to calculate the corrected MeHg concentrations according to Eq. (4). The resulting concentrations, methylation factors ($F_{methylation}$), and corrections are displayed in Table 2. As a comparison, the MeHg concentrations measured with a classical set of standards methods are displayed. Generally, the MeHg concentrations from isotopic dilution analyses (IDA) were higher when compared to the set of standard method or certified values. This shows that MeHg is overestimated during IDA experiment as previously reported (Monperrus et al., 2008). Methylation factors ($F_{methylation}$) ranged between 0.0072 and 0.033%, were sample specific, and were similar to other published $F_{methylation}$ using acid-leaching organic solvent extraction procedures (Hintelman et al., 1997). However, these corrections only account for the methylation of iHg and do not cover the net MeHg production including the potential demethylation. The results of MeHg concentrations from DSIDA were generally higher than the results from the set of standards calibrations (Table 2) but were in the same range after correction according to Eq. (4).

Table 2
Experimentally determined methylation factors from species specific double spike isotope dilution (Experiment A) and corrected concentrations for isotope dilution analyses.

Sample	Experiment	Quantification Method	Hg_{HNO3} (μg/g)	Hg_{HCl} (μg/g)	$MeHg_{analyzed}$ (ng/g)	MeHg formation			
						$MeHg_{corrected}$ (ng/g)	$F_{methylation}$ (%)	MeHg formed (ng/g)	Resulting error (%)
	Acid leaching	Set of Standards		78.1 ± 2.9					
ERM CC580	Isotope dilution	IDA			99 ± 1	73 ± 2	0.033 ± 0.001	26 ± 1.2	35
	Extraction	Set of Standards			68 ± 2				
	Certified Value		132 ± 3		75 ± 4				
Canal Site (one sample)	Acid leaching	Set of Standards	41 ± 2	32 ± 2					
	Isotope dilution	IDA			2.75 ± 0.07	1.20 ± 0.02	0.0048 ± 0.0003	1.56 ± 0.08	130
	Extraction	Set of Standards			1.9 ± 0.1				
Landfill Site (one sample)	Acid leaching	Set of Standards	60 ± 3	53 ± 1					
	Isotope dilution	IDA			16.9 ± 0.4	13.1 ± 0.5	0.0072 ± 0.0006	3.8 ± 0.3	29
	Extraction	Set of Standards			11.2 ± 0.5				
Hot Spot Site (one sample)	Acid leaching	Set of Standards	0.72 ± 0.04	0.72 ± 0.03					
	Isotope dilution	IDA			2.9 ± 0.1	2.7 ± 0.1	0.03 ± 0.02	0.23 ± 0.17	9
	Extraction	Set of Standards			2.2 ± 0.1	2.2 ± 0.1			

3.2.2. *Experiment B - artificial methylation: spiking of iHg^{2+}*

In experiment B, blanks, two soil samples from our inhouse sample bank and the CRM ERM CC-580 were spiked with iHg. We observed linear relationships between the amount of iHg in HCl and that of MeHg present after extraction (Fig. 3), where the slope for each linear model (Eq. (3)) represents the factor of MeHg produced from iHg. Table 3 shows the methylation factors and regression coefficients for the linear regressions of all experimental runs. Methylation factors are consistent within the tested soil and sediment matrices (0.0075%) and are within the same order of magnitude as that using 5 mol L^{-1} HCl and toluene as extraction solvent (0.005%) from Hintelman et al. (1997). This contrasts with the results from IDA where $F_{methylation}$ was sample-specific. However, Hg^{2+} spiking allowed for an evaluation of net MeHg production for Hg^{2+} in the extract. The $F_{methylation}$ of the Hg^{2+} spiking experiments represents net MeHg production during sample extraction. The data further suggests that $F_{methylation}$ is sample-independent.

The highest factors of MeHg produced from iHg were observed in the experiments where blanks were only spiked with iHg^{2+} (Table S8; Fig. 3). This suggests that CH_2Cl_2 acts as the source of C for iHg methylation during the extraction procedure. Based on earlier studies, we assumed that an iHg spike behaves similar to ambient Hg during acid extraction (Liang et al., 2004). Our results are in disagreement with Hintelman et al. (1997) who observed methylation only during the HCl leaching step, but none during the extraction step with the organic solvent (toluene). They concluded that mainly soil and sediment constituents were responsible for the artificial formation of MeHg. Here, we show evidence that the abiotic methylation of iHg took place with CH_2Cl_2 as the C source. In the future, this information should be considered during the development of MeHg extraction procedures. The presence of MeHg in the added iHg standard can be ruled out as this high purity standard is back-traced to a metallic Hg standard by the producer and kept in 12% HNO_3. Further, the lower $F_{methylation}$ for soil matrices suggests that the constituents of sediments and soils may passivate iHg^{2+} (e.g., by complexing) and make it less prone to artificial methylation during the HCl–CH_2Cl_2 extraction.

In any case, soil samples from contaminated sites are often reported to have MeHg/Hg ratios ≪ 0.01%. It cannot be emphasized enough that even a small percentage of artificial methylation (<0.01%) may result in false positives that account for >60% of the MeHg concentration in a sample (Table 3). Thus, reports of uncommonly high MeHg concentrations in polluted areas should always be interpreted with caution if MeHg was extracted by acid-leaching and organic solvents (Gray et al.,

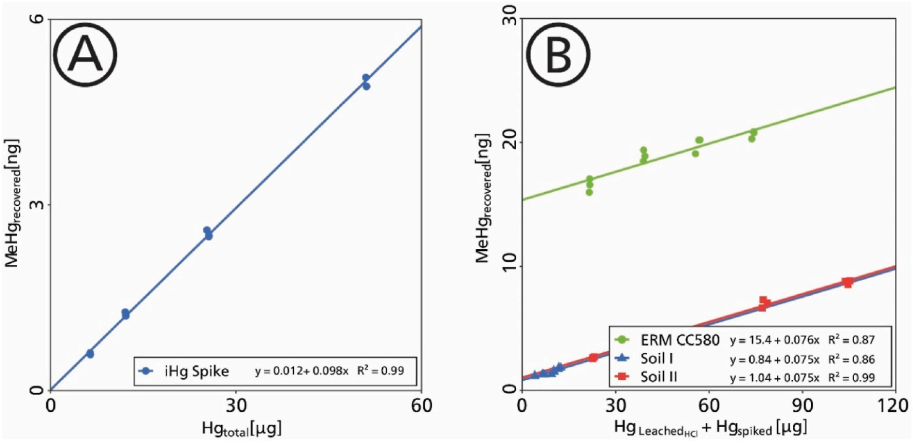

Fig. 3. Amount of MeHg [ng] recovered from HCl/CH_2Cl_2 extraction as a function of A) spiked iHg [μg] to a blank sample B) spiked iHg and HCl leached Hg [μg] of 250 mg sample material. Functions displayed show linear regressions of the specific runs. Experimental replicates (n = 3) are displayed as individual points.

Table 3
Experimentally determined methylation factors ($F_{methylation}$) calculated from spiking of iHg (Experiment B).

Sample Type	Name	Hg μg g^{-1}	$Hg_{leached(HCl)}$ μg g^{-1}	MeHg ng g^{-1}	$F_{methylation}$ %	Artificial MeHg ng g^{-1}	Resulting error %
iHg spike	–	10	10	–	0.00980	9.8	100
Sediment	ERM-CC580	132 ± 3[a]	86 ± 2	75 ± 4	0.00756	6.5	9
Soil	Soil I	21 ± 1	15.8 ± 0.2	4.99 ± 0.09	0.00749	1.2	24
Soil	Soil II	193 ± 2	91 ± 3	11.4 ± 0.2	0.00748	7	60

[a] Certified concentrations taken from the certificate of the respective CRM.

2004; Kodamatani et al., 2022). Our results call for the correction of artificially formed MeHg in samples with elevated Hg concentrations by using Eq. (4). The requirements for this approximation include an analysis of 1) concentrations of extracted MeHg, 2) Hg leached by HCl (1st step of the extraction procedure) and 3) calculating $F_{methlyation}$ for a specific extraction procedure. Although the correction is straight forward, the correction factors still must be interpreted with caution, since the exact reactions or mechanisms of the artificial methylation are still unclear.

For the CRM ERM CC-580 the correction resulted in a concentration of 62 ± 2 μg kg^{-1} (n = 39) representing a recovery of 82 ± 3% compared to the certified concentration. The uncorrected recovery was 91 ± 3% and does not reflect the actual performance of the applied method. This CRM is one of few materials certified for MeHg (Leermakers et al., 2003). Its properties differ in many aspects (e.g. organic matter or carbonate content) from our target sample matrix. The use of a dissimilar CRM may be deceptive when assessing the effectiveness of an extraction procedure since artificial MeHg formation might 1) result as a misinterpretation of the performance and 2) be sample-specific and not comparable to the study's target sample matrices. MeHg artifact formation was often reported to depend on substrate properties (e.g., organic matter, pH or Hg speciation) (Bloom et al., 1997; Hammerschmidt and Fitzgerald, 2001; Falter, 1999b; Hintelman et al., 1997). It is therefore crucial to increase the availability of new soil CRMs with high Hg and certified MeHg concentrations to help in the development of suitable methods for MeHg determination in soils. Producers of these materials emphasize the diversity of substrate properties (pH, organic matter or Hg speciation etc.).

3.3. Distribution of organic Hg species in the sites

For the sampled soils of the field campaign, uncorrected MeHg concentrations significantly correlate to HgT in both canal ($R^2 = 0.5$, $p < 0.05$) and landfill ($R^2 = 0.66$, $p < 0.05$) sites (Fig. S9). This indicates that the MeHg analyses were affected by MeHg artifact formation since, in contaminated soils (>2 mg kg^{-1} Hg), MeHg/Hg ratios were generally <0.1%. Thus, we applied the mean $F_{methylation}$ of ERM CC-580, Soil 1, and Soil 2 (0.0075%) and Eq. (4) to correct the MeHg concentrations in the field study. The site-specific HCl-leachable percentage was measured by ICP-MS on a selection of samples per site (Fig. S13). For each sampling site, the specific HCl-leachable percentages were multiplied by the HgT concentration to obtain an estimate of HCl-leachable Hg. The corrections resulted in 27 out of 163 samples with negative MeHg concentrations indicating an overestimation of HCl leachable Hg or the $F_{methylation}$. For the rest of the manuscript, they are treated as samples < LoD (0.16 μg kg^{-1}).

The $MeHg_{corrected}$ values in the different soil profiles are displayed in Fig. 1. At the canal site, MeHg had no distinct spatial trend. The highest concentrations (5.8 μg kg^{-1}) were detected at a 20 m distance from the canal (Fig. 1). No EtHg was detected at this site. The mean $MeHg_{corrected}$ values continuously decrease with soil depth with no horizontal trends at the landfill site. At the hotspot site, $MeHg_{corrected}$ concentrations range from 0.8 to 9.8 μg kg^{-1}. High $MeHg_{corrected}$ concentrations do not necessarily correlate to high Hg concentrations.

The uncorrected MeHg concentration is the only parameter showing a positive correlation ($R^2 > 0.75$, $p < 0.05$) to the $MeHg_{corrected}$ concentrations (Fig. S9). This suggests that neither textural nor chemical soil properties were governing MeHg concentrations in the sampled soils. Different factors may be more important including changing redox conditions (Gfeller et al., 2021), the presence of Hg methylating or demethylating microorganisms (carrying *hgcAB complex* or *merA/B* genes, respectively), or an external source of MeHg.

The presence of the *hgcA* gene was detected after PCR amplification in 8 out of 9 samples of the regularly flooded canal site (Fig. 4). The elevated rate of *hgcA* gene presence in addition to the observed regular redox oscillations (Gfeller et al., 2021) indicates that soils at the canal site have a high potential for Hg biomethylation (Fig. 4). We suggest that MeHg is mainly produced *in situ* at this site, which is in line with our previous work (Gygax et al., 2019 and Gfeller et al., 2021) where we demonstrated a positive net methylation potential of these soils in microcosm experiments. However, the abundance of the *hgcA* gene does not imply higher MeHg concentrations (Liu et al., 2018; Christensen et al., 2019). This is not surprising since Hg biomethylation is a dynamic process governed by 1) the soil chemistry, 2) the activity and expression of the two-gene cluster (*hgcAB*) and 3) site-specific redox dynamics. Landfill and hot spot sites only showed positive signals for *hgcA* in 1 out of a total of 14 samples (Fig. 4). We hypothesize that the absence of *hgcA* is an indication of low to no biomethylation processes in the soil, which, combined with elevated MeHg levels, suggests an anthropogenic source of MeHg.

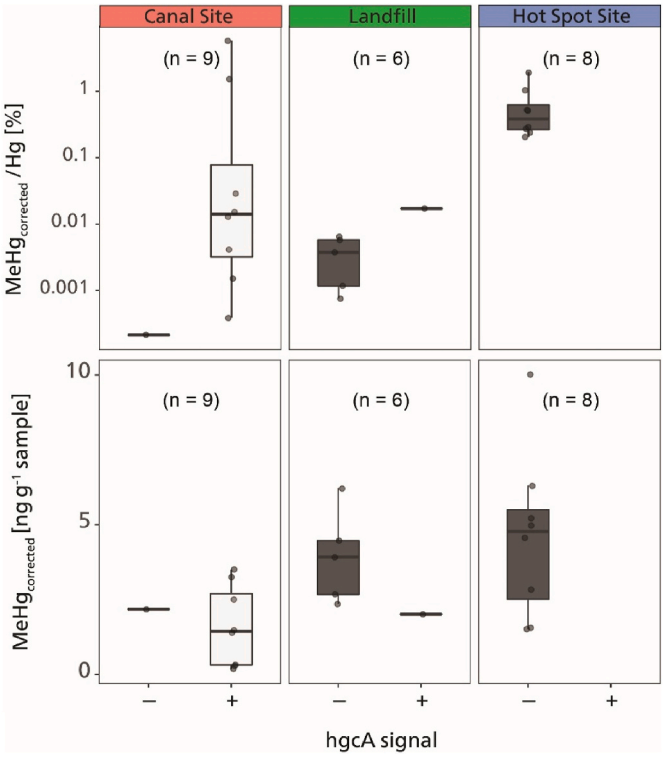

Fig. 4. Boxplots displaying concentration and MeHg/Hg ratios for the samples analyzed for hgcA at each sampling sites. Data is aggregated by hgcA positive resp. negative signals.

EtHg was detected in 11 samples at the landfill site and 5 samples at the hotspot site but was not detected at the canal site. At the hotspot site, EtHg was only detected in the core with the highest Hg concentrations (91–245 mg kg^{-1}). No spatial pattern was found in the landfill site. In the samples where EtHg was detected, the concentrations were between 0.14 and 0.47 μg kg^{-1}. EtHg concentrations should be interpreted as minima since EtHg degrades relatively fast under our extraction conditions (Han et al., 2003; Hight and Cheng, 2006). EtHg concentrations were 2-fold lower than the EtHg concentrations measured in a smelter site in Slovenia (Tomiyasu et al., 2017), but were within the range of EtHg measured in a remote area in the Everglades in Florida (Mao et al., 2010). To our knowledge, no systematic studies showed that EtHg is formed quantitively in the environment and EtHg formation pathway(s) remain unstudied in soils or sediments. It appears more likely that EtHg in soils comes from an anthropogenic source when detected close to industrial legacy sites. Elevated levels of EtHg at chlor-alkali and acetaldehyde producing legacy sites have been attributed to side products of the chemical industry (Hintelman et al., 1995; Tomiyasu et al., 2017).

The pollution history in our study area remains complex since contaminated soils and sediments were reportedly transported and redistributed (e.g., as fill material) and no exhaustive documentation exists on these events (Glenz and Escher, 2011; Mudry, 2016). We suggest that organic Hg species in both hotspot and landfill sites were directly emitted from the chemical plant, and not produced post-deposition. The line of evidence consists of 1) the detection of EtHg, 2) the elevated MeHg concentrations (up to 4.84 μg kg^{-1}), and 3) the absence of the *hgcA* gene. We suggest that the directly deposited MeHg is as well demethylated through time. This hypothesis is supported by Osterwalder et al. (2019), who found that the abundance of the *mer*-operon in soil DNA linearly increased with Hg concentrations in our study area and the missing correlation between MeHg and Hg at our study sites. At the canal site, Hg contamination is well documented and mainly originates from the canal sediments deposited on the canal's bank (Glenz and Escher, 2011). There, soil MeHg may not be fully attributed to either anthropogenic emissions or biological activity. These soils are subjected to regular redox oscillations, show net methylation potential (Gfeller et al., 2021; Gygax et al., 2019) and present *hgcA* genes.

4. Conclusions

We sampled soil from three sites in a contaminated agricultural floodplain in the canton of Valais, Switzerland. The soils in all three sites showed high concentrations of Hg correlating with those of Cu and Pb, indicating a common contamination source. The pollution history was only well documented for one site (canal), while missing for the other two (landfill and hotspot). We used and improved organic Hg speciation method to further understand the local pollution at these sites.

Our results are in agreement with earlier studies reporting artificial MeHg formation during MeHg extraction with HCl–Cl_2CH_2 and we observed consistent methylation rates ($F_{methylation}$ = (0.0075 ± 0.0001%) throughout different sample types. These rates were consistent with previously published acid-leaching solvent extraction procedures. Although small, the methylation rates were demonstrated to be relevant for Hg polluted soil or sediment samples with low MeHg/Hg ratios resulting in false positives of >60% of the analyte concentration (Table 3). We are not aware of neither an artifact-free extraction method nor suitable soil CRM to overcome these limitations in the study of MeHg dynamics in highly Hg polluted soils. Therefore, it is of utmost importance for the scientific community to develop suitable extraction methods and reference materials.

We used the determined methylation factor to correct for false positives in the above-mentioned field campaign. The detection of MeHg and EtHg, as well as the absence of the *hgcA* genes, served as evidence to conclude that these organic Hg species were directly emitted by the chemical plant. Although, these circumstances are rather coincidental since the change in environmental conditions (e.g., flooding of soils) might ultimately result in a change of microbial communities and consequently blur the grounds for our conclusions. Organic Hg speciation and methylation gene (hgcA) abundance analyses are strongly complementing classic methods (e.g., literature research and interviews with stakeholders) when assessing the pollution history of a legacy site.

Financial support

This work was funded by the Swiss National Science Foundation [SNSF, grant no. 163661].

Author contribution

Adrien Mestrot and Lorenz Gfeller designed the study. Lorenz Gfeller, Jaime N. Caplette and Adrien Mestrot performed the field sampling. Lorenz Gfeller, Aline Frossard and Jaime N. Caplette performed laboratory analyses. Lorenz Gfeller performed the data analysis. Adrien Mestrot and Aline Frossard supervised the study. Adrien Mestrot financed the study. Lorenz Gfeller prepared the manuscript with contributions from all co-authors.

Declaration of competing interest

The authors declare that they have no known competing financial interests or personal relationships that could have appeared to influence the work reported in this paper.

Data availability

Data will be made available on request.

Acknowledgements

We acknowledge Patrick Neuhaus and Daniela Fischer for the help in the laboratory in Bern. We thank Beat Stierli and Beat Frey for the DNA extraction and the PCR at the Federal Research Institute WSL and Stephane Westermann at the Dienststelle für Umweltschutz (DUS) of the Canton Wallis for the help with site selection and sampling permissions. Milena Horvat's group at Institute Jozef Stefan, Slovenia is acknowledged for providing an ethyl mercury standard material. Emmanuel Tessier and David Amouroux are thanked for the valuable advice concerning isotopic dilution. Teresa González de Chávez Capilla and Moritz Bigalke of the soil science group at the Institute of Geography at University of Bern gave valuable advice during the writing process.

Appendix A. Supplementary data

Supplementary data to this article can be found online at https://doi.org/10.1016/j.envpol.2022.119854.

References

AMAP/UN Environment, Arctic Monitoring and Assessment Programme, UN Environment Programme, 2019. Technical Background Report for the Global Mercury Assessment 2018. Arctic Monitoring and Assessment Programme, Oslo, Norway/UN Environment Programme, Chemicals and Health Branch, Geneva, Switzerland 1–426.

Amos, H.M., Jacob, D.J., Streets, D.G., Sunderland, E.M., 2013. Legacy impacts of all-time anthropogenic emissions on the global mercury cycle. Global Biogeochem. Cycles 27, 410–421. https://doi.org/10.1002/gbc.20040.

Bigham, G.N., Murray, K.J., Masue-Slowey, Y., Henry, E.A., 2017. Biogeochemical controls on methylmercury in soils and sediments: implications for site management. Integrated Environ. Assess. Manag. 13, 249–263. https://doi.org/10.1002/ieam.1822.

Bloom, N.S., Colman, J.A., Barber, L., 1997. Artifact formation of methyl mercury during aqueous distillation and alternative techniques for the extraction of methyl mercury from environmental samples. Fresen. J. Anal. Chem. 371–377.

Brombach, C.-C., Gajdosechova, Z., Chen, B., Brownlow, A., Corns, W.T., Feldmann, J., Krupp, E.M., 2015. Direct online HPLC-CV-AFS method for traces of methylmercury

without derivatisation: a matrix-independent method for urine, sediment and biological tissue samples. Anal. Bioanal. Chem. 407, 973–981. https://doi.org/10.1007/s00216-014-8254-1.

Christensen, G.A., Gionfriddo, C.M., King, A.J., Moberly, J.G., Miller, C.L., Somenahally, A.C., Callister, S.J., Brewer, H., Podar, M., Brown, S.D., Palumbo, A.V., Brandt, C.C., Wymore, A.M., Brooks, S.C., Hwang, C., Fields, M.W., Wall, J.D., Gilmour, C.C., Elias, D.A., 2019. Determining the reliability of measuring mercury cycling gene abundance with correlations with mercury and methylmercury concentrations. Environ. Sci. Technol. 53, 8649–8663. https://doi.org/10.1021/acs.est.8b06389.

Driscoll, C.T., Mason, R.P., Chan, H.M., Jacob, D.J., Pirrone, N., 2013. Mercury as a global pollutant: sources, pathways, and effects. Environ. Sci. Technol. 47, 4967–4983. https://doi.org/10.1021/es305071v.

Duan, Y., Han, D.S., Batchelor, B., Abdel-Wahab, A., 2016. Synthesis, characterization, and application of pyrite for removal of mercury. Colloids Surf. A Physicochem. Eng. Asp. 490, 326–335. https://doi.org/10.1016/j.colsurfa.2015.11.057.

Falter, R., 1999a. Experimental study on the unintentional abiotic methylation of inorganic mercury during analysis: Part 1: localisation of the compounds effecting the abiotic mercury methylation. Chemosphere 39, 1051–1073. https://doi.org/10.1016/S0045-6535(99)00178-2.

Falter, R., 1999b. Experimental study on the unintentional abiotic methylation of inorganic mercury during analysis: Part 2: controlled laboratory experiments to elucidate the mechanism and critical discussion of the species specific isotope addition correction method. Chemosphere 39, 1075–1091. https://doi.org/10.1016/S0045-6535(99)00179-4.

Frossard, A., Donhauser, J., Mestrot, A., Gygax, S., Bååth, E., Frey, B., 2018. Long- and short-term effects of mercury pollution on the soil microbiome. Soil Biol. Biochem. 120, 191–199. https://doi.org/10.1016/j.soilbio.2018.01.028.

Gfeller, L., Weber, A., Worms, I., Slaveykova, V.I., Mestrot, A., 2021. Mercury mobility, colloid formation and methylation in a polluted Fluvisol as affected by manure application and flooding–draining cycle. Biogeosciences 18, 3445–3465. https://doi.org/10.5194/bg-18-3445-2021.

Gilli, R., Karlen, C., Weber, M., Rüegg, J., Barmettler, K., Biester, H., Boivin, P., Kretzschmar, R., 2018. Speciation and mobility of mercury in soils contaminated by legacy emissions from a chemical factory in the rhône valley in canton of Valais, Switzerland. Soil Systems 2, 44. https://doi.org/10.3390/soilsystems2030044.

Glenz, C., Escher, J.-R., 2011. Voruntersuchung von belasteten Standorten: Historische Untersuchung Objekt Grossgrundkanal, vol. 89. FUAG-Forum Umwelt AG, Visp, Switzerland.

Gray, J.E., Hines, M.E., Higueras, P.L., Adatto, I., Lasorsa, B.K., 2004. Mercury speciation and microbial transformations in mine wastes, stream sediments, and surface waters at the Almadén Mining District, Spain. Environ. Sci. Technol. 38, 4285–4292. https://doi.org/10.1021/es040359d.

Grégoire, D.S., Poulain, A.J., 2018. Shining light on recent advances in microbial mercury cycling. FACETS 3, 858–879. https://doi.org/10.1139/facets-2018-0015.

Grigg, A.R.C., Kretzschmar, R., Gilli, R.S., Wiederhold, J.G., 2018. Mercury isotope signatures of digests and sequential extracts from industrially contaminated soils and sediments. Sci. Total Environ. 636, 1344–1354. https://doi.org/10.1016/j.scitotenv.2018.04.261.

Gygax, S., Gfeller, L., Wilcke, W., Mestrot, A., 2019. Emerging investigator series: mercury mobility and methylmercury formation in a contaminated agricultural flood plain: influence of flooding and manure addition. Environ. Sci. Process. Impacts 21, 2008–2019. https://doi.org/10.1039/c9em00257j.

Hammerschmidt, C.R., Fitzgerald, W.F., 2001. formation of artifact methylmercury during extraction from a sediment reference material. Anal. Chem. 73, 5930–5936. https://doi.org/10.1021/ac010721w.

Han, Y., Kingston, H.M., Boylan, H.M., Rahman, G.M.M., Shah, S., Richter, R.C., Link, D. D., Bhandari, S., 2003. Speciation of mercury in soil and sediment by selective solvent and acid extraction. Anal. Bioanal. Chem. 375, 428–436. https://doi.org/10.1007/s00216-002-1701-4.

Hellmann, C., Costa, R.D., Schmitz, O.J., 2019. How to deal with mercury in sediments? A critical review about used methods for the speciation of mercury in sediments. Chromatographia 82, 125–141. https://doi.org/10.1007/s10337-018-3625-y.

Hight, S.C., Cheng, J., 2006. Determination of methylmercury and estimation of total mercury in seafood using high performance liquid chromatography (HPLC) and inductively coupled plasma-mass spectrometry (ICP-MS): method development and validation. Anal. Chim. Acta 567, 160–172. https://doi.org/10.1016/j.aca.2006.03.048.

Hintelman, H., Falter, R., Ilgen, G., Evans, D.R., 1997. Determination of artifactual formation of monomethylmercury (CH3Hg+) in environmental samples using stable Hg2+ isotopes with ICP-MS detection: calculation of contents applying species specific isotope addition. Fresen. J. Anal. Chem. 358, 363–370.

Hintelman, H., Hempel, M., Wilken, R.-D., 1995. Observation of unusual organic mercury species in soils and sediments of industrially contaminated sites. Environ. Sci. Technol. 29, 1845–1850.

Hojdová, M., Rohovec, J., Chrastný, V., Penížek, V., Navrátil, T., 2015. The influence of sample drying procedures on mercury concentrations analyzed in soils. Bull. Environ. Contam. Toxicol. 94, 570–576. https://doi.org/10.1007/s00128-015-1521-9.

Horowitz, H.M., Jacob, D.J., Amos, H.M., Streets, D.G., Sunderland, E.M., 2014. Historical Mercury releases from commercial products: global environmental implications. Environ. Sci. Technol. 48, 10242–10250. https://doi.org/10.1021/es501337j.

Horvat, M., Liang, L., Bloom, N.S., 1993. Comparison of distillation with other current isolation methods for the determination of methyl mercury compounds in low level environmental samples. Anal. Chim. Acta 282, 153–168. https://doi.org/10.1016/0003-2670(93)80364-Q.

Huang, J.-H., 2005. Artifact formation of methyl- and ethyl-mercury compounds from inorganic mercury during derivatization using sodium tetra(n-propyl)borate. Anal. Chim. Acta 532, 113–120. https://doi.org/10.1016/j.aca.2004.10.057.

Imseng, M., Wiggenhauser, M., Müller, M., Keller, A., Frossard, E., Wilcke, W., Bigalke, M., 2019. The fate of Zn in agricultural soils: a stable isotope approach to anthropogenic impact, soil formation, and soil-plant cycling. Environ. Sci. Technol. 53, 4140–4149. https://doi.org/10.1021/acs.est.8b03675.

IUSS Working Group WRB, 2015. World Reference Base for Soil Resources 2014, Update 2015: International Soil Classification System for Naming Soils and Creating Legends for Soil Maps, vol. 106. Food and Agriculture Organization of the United Nations, Rome, p. 203. World Soil Resources Reports.

Jagtap, R., Maher, W., 2015. Measurement of mercury species in sediments and soils by HPLC–ICPMS. Microchem. J. 121, 65–98. https://doi.org/10.1016/j.microc.2015.01.010.

Jonsson, S., Skyllberg, U., Nilsson, M.B., Westlund, P.-O., Shchukarev, A., Lundberg, E., Björn, E., 2012. Mercury methylation rates for geochemically relevant Hg(II) species in sediments. Environ. Sci. Technol. 46, 11653–11659. https://doi.org/10.1021/es3015327.

Kodamatani, H., Shigetomi, A., Akama, J., Kanzaki, R., Tomiyasu, T., 2022. Distribution, alkylation, and migration of mercury in soil discharged from the Itomuka mercury mine. Sci. Total Environ. 815, 152492 https://doi.org/10.1016/j.scitotenv.2021.152492.

Lazareva, O., Sparks, D.L., Landis, R., Ptacek, C.J., Ma, J., 2019. Investigation of legacy industrial mercury in floodplain soils: south River, Virginia, USA. Environ. Earth Sci. 78, 276. https://doi.org/10.1007/s12665-019-8253-9.

Leermakers, M., Nguyen, H.L., Kurunczi, S., Vanneste, B., Galletti, S., Baeyens, W., 2003. Determination of methylmercury in environmental samples using static headspace gas chromatography and atomic fluorescence detection after aqueous phase ethylation. Anal. Bioanal. Chem. 377, 327–333. https://doi.org/10.1007/s00216-003-2116-6.

Liang, L., Horvat, M., Feng, X., Shang, L., Li, H., Pang, P., 2004. Re-evaluation of distillation and comparison with HNO3 leaching/solvent extraction for isolation of methylmercury compounds from sediment/soil samples. Appl. Organomet. Chem. 18, 264–270. https://doi.org/10.1002/aoc.617.

Liu, Y.-R., Johs, A., Bi, L., Lu, X., Hu, H.-W., Sun, D., He, J.-Z., Gu, B., 2018. Unraveling microbial communities associated with methylmercury production in paddy soils. Environ. Sci. Technol. 52, 13110–13118. https://doi.org/10.1021/acs.est.8b03052.

Mantovi, P., Bonazzi, G., Maestri, E., Marmiroli, N., 2003. Accumulation of copper and zinc from liquid manure in agricultural soils and crop plants. Plant Soil 250, 249–257. https://doi.org/10.1023/A:1022848131043.

Mao, Y., Yin, Y., Li, Y., Liu, G., Feng, X., Jiang, G., Cai, Y., 2010. Occurrence of monoethylmercury in the Florida Everglades: identification and verification. Environ. Pollut. 158, 3378–3384. https://doi.org/10.1016/j.envpol.2010.07.031.

Marvin-DiPasquale, M., Windham-Myers, L., Agee, J.L., Kakouros, E., Le Kieu, H., Fleck, J.A., Alpers, C.N., Stricker, C.A., 2014. Methylmercury production in sediment from agricultural and non-agricultural wetlands in the Yolo Bypass, California, USA. Sci. Total Environ. 484, 288–299. https://doi.org/10.1016/j.scitotenv.2013.09.098.

Matsumoto, H., Koya, G., Takeuchi, T., 1965. Fetal minamata disease: a neuropathological study of two cases of intrauterine intoxi cation by a methyl mercury compound. JNEN (J. Neuropathol. Exp. Neurol.) 24, 563–574. https://doi.org/10.1097/00005072-196510000-00002.

Monperrus, M., Krupp, E., Amouroux, D., Donard, O., Rodriguez Martin-Doimeadios, R., 2004. Potential and limits of speciated isotope-dilution analysis for metrology and assessing environmental reactivity. TrAC Trends Anal. Chem. (Reference Ed.) 23, 261–272. https://doi.org/10.1016/S0165-9936(04)00313-9.

Monperrus, M., Rodriguez Gonzalez, P., Amouroux, D., Garcia Alonso, J.I., Donard, O.F. X., 2008. Evaluating the potential and limitations of double-spiking species-specific isotope dilution analysis for the accurate quantification of mercury species in different environmental matrices. Anal. Bioanal. Chem. 390, 655–666. https://doi.org/10.1007/s00216-007-1598-z.

Mudry, A., 2016. Quecksilberbelastungen im Raum Visp - Niedergesteln: Weitere Ergebnisse im Siedlungsgebiet, vol. 2. Sion.

Nagase, H., Ose, Y., Sato, T., Ishikawa, T., 1984. Mercury methylation by compounds in humic material. Sci. Total Environ. 32, 147–156. https://doi.org/10.1016/0048-9697(84)90127-X.

Osterwalder, S., Huang, J.-H., Shetaya, W.H., Agnan, Y., Frossard, A., Frey, B., Alewell, C., Kretzschmar, R., Biester, H., Obrist, D., 2019. Mercury emission from industrially contaminated soils in relation to chemical, microbial, and meteorological factors. Environ. Pollut. 250, 944–952. https://doi.org/10.1016/j.envpol.2019.03.093.

Panagos, P., Jiskra, M., Borrelli, P., Liakos, L., Ballabio, C., 2021. Mercury in European topsoils: anthropogenic sources, stocks and fluxes. Environ. Res. 201, 111556–111567. https://doi.org/10.1016/j.envres.2021.111556.

Parks, J.M., Guo, H., Momany, C., Liang, L., Miller, S.M., Summers, A.O., Smith, J.C., 2009. Mechanism of Hg-C protonolysis in the organomercurial lyase MerB. J. Am. Chem. Soc. 131, 13278–13285. https://doi.org/10.1021/ja9016123.

Parks, J.M., Johs, A., Podar, M., Bridou, R., Hurt, R.A.[., Smith, S.D., Tomanicek, S.J., Qian, Y., Brown, S.D., Brandt, C.C., Palumbo, A.V., Smith, J.C., Wall, J.D., Elias, D. A., Liang, L., 2013. The genetic basis for bacterial mercury methylation. Science 339, 1332–1335.

Podar, M., Gilmour, C.C., Brandt, C.C., Soren, A., Brown, S.D., Crable, B.R., Palumbo, A. V., Somenahally, A.C., Elias, D.A., 2015. Global prevalence and distribution of genes and microorganisms involved in mercury methylation. Sci. Adv. 1, e1500675 https://doi.org/10.1126/sciadv.1500675.

Poulain, A.J., Barkay, T., 2013. Cracking the mercury methylation code. Science 339, 1280–1281. https://doi.org/10.1126/science.1235591.

Quenvauviller, P., Horvat, M., 1999. Letter to the Editor: artifact formation of methylmercury in sediments. Anal. Chem. 71, 155A. https://doi.org/10.1021/ac990222j.

Qvarnström, J., Frech, W., 2002. Mercury species transformations during sample pretreatment of biological tissues studied by HPLC-ICP-MS. J. Anal. At. Spectrom. 17, 1486–1491. https://doi.org/10.1039/B205246F.

Rogers, R.D., 1976. Methylation of mercury in agricultural soils. J. Environ. Qual. 5, 454–458. https://doi.org/10.2134/jeq1976.00472425000500040028x.

Rogers, R.D., 1977. Abiological methylation of mercury in soil. J. Environ. Qual. 6, 463–467. https://doi.org/10.2134/jeq1977.00472425000600040029x.

RStudio Team, 2020. RStudio: Integrated Development for R., RStudio Team. PBC, Boston, MA.

Sannac, S., Chen, Y.-H., Wahlen, R., McCurdy, E., Agilent Technologies, 2017. Benefits of HPLC-ICP-MS coupling for mercury speciation in food: application note. Agilent Application Notes 1–6, 5991-0066EN.

Sannac, S., Fisicaro, P., Labarraque, G., Pannier, F., Potin-Gautier, M., 2009. Development of a reference measurement procedure for the determination of methylmercury in fish products. Accred Qual. Assur. 14, 263–267. https://doi.org/10.1007/s00769-009-0509-8.

Singer, M.B., Harrison, L.R., Donovan, P.M., Blum, J.D., Marvin-DiPasquale, M., 2016. Hydrologic indicators of hot spots and hot moments of mercury methylation potential along river corridors. Sci. Total Environ. 568, 697–711. https://doi.org/10.1016/j.scitotenv.2016.03.005.

Tomiyasu, T., Kodamatani, H., Imura, R., Matsuyama, A., Miyamoto, J., Akagi, H., Kocman, D., Kotnik, J., Fajon, V., Horvat, M., 2017. The dynamics of mercury near Idrija mercury mine, Slovenia: horizontal and vertical distributions of total, methyl, and ethyl mercury concentrations in soils. Chemosphere 184, 244–252. https://doi.org/10.1016/j.chemosphere.2017.05.123.

Wang, B., Zhong, S., Bishop, K., Nilsson, M.B., Hu, H., Eklöf, K., Bravo, A.G., Åkerblom, S., Bertilsson, S., Björn, E., Skyllberg, U., 2021. Biogeochemical influences on net methylmercury formation proxies along a peatland chronosequence. Geochem. Cosmochim. Acta 308, 188–203. https://doi.org/10.1016/j.gca.2021.06.010.

Wilken, R.-D., Nitschke, F., Falter, R., 2003. Possible interferences of mercury sulfur compounds with ethylated and methylated mercury species using HPLC-ICP-MS. Anal. Bioanal. Chem. 377, 149–153. https://doi.org/10.1007/s00216-003-2090-z.

Windham-Myers, L., Marvin-DiPasquale, M., Kakouros, E., Agee, J.L., Le Kieu, H., Stricker, C.A., Fleck, J.A., Ackerman, J.T., 2014. Mercury cycling in agricultural and managed wetlands of California, USA: seasonal influences of vegetation on mercury methylation, storage, and transport. Sci. Total Environ. 484, 308–318. https://doi.org/10.1016/j.scitotenv.2013.05.027.

Xu, Xiaohang, Lin, Yan, Meng, Bo, Feng, Xinbin, Xu, Zhidong, Jiang, Yuping, Zhong, Weilu, Hu, Yanhai, Qiu, Guangle, 2018. The impact of an abandoned mercury mine on the environment in the Xiushan region, Chongqing, southwestern China. Appl. Geochem. 88, 267–275. https://doi.org/10.1016/j.apgeochem.2017.04.005. S0883292717300410.

Zhang, T., Kucharzyk, K.H., Kim, B., Deshusses, M.A., Hsu-Kim, H., 2014. Net methylation of mercury in estuarine sediment microcosms amended with dissolved, nanoparticulate, and microparticulate mercuric sulfides. Environ. Sci. Technol. 48, 9133–9141. https://doi.org/10.1021/es500336j.

Zhang, Y., Liu, Y.-R., Lei, P., Wang, Y.-J., Zhong, H., 2018. Biochar and nitrate reduce risk of methylmercury in soils under straw amendment. Sci. Total Environ. 619–620, 384–390. https://doi.org/10.1016/j.scitotenv.2017.11.106.